Long Ago, in a Globular Cluster Far, Far Away: Discovering the Secrets of the Universe with the Messier 13 Globular Cluster

Claire Thomas, Izabella Gurreonero, Keira Seidman, Lihini Ranaweera, Thomas Hasty

Abstract

Globular clusters are a type of celestial object that can be used to provide insight into the history of the universe. Using a telescope housed at University of Pittsburgh's Allegheny Observatory, we imaged the globular cluster M13 to determine its age. By using images of M13 taken in different telescope filters, in conjunction with bias and flat calibration frames, we calculated the absolute magnitudes of 900+ stars in the cluster and used this information to create a Hertzsprung-Russell diagram (H-R diagram) for M13. With the data from the H-R diagram we were able to consult an isochrone chart to determine the age of M13. We also imaged various other celestial objects and used three gray-scale images of them taken with different filters to create three-color images and we describe the different structures of galaxies and various other astronomical phenomena that may have impacted our data. Using these techniques, we discover that the insights gained from studying globular clusters contribute to a deeper understanding of the universe.

I. Introduction

A. What are Globular Clusters?

1. Introduction to Star Clusters

The universe remains vast and mostly unexplored, with experts only having discovered a meager four percent of the apparent space. To compensate for our lack of knowledge, astronomers aim to use star clusters to chart the interaction between galaxies and make new discoveries about the nature of our universe. Within our research, there are two different types of star clusters which were discussed: open clusters and globular clusters

2. Globular clusters vs. Open Clusters

Open clusters are much smaller than globular clusters. These types of star clusters are scattered throughout the disk of our galaxy and presumably numerous others which have yet to be explored. Open clusters contain between a few dozen and a few thousand stars, which are all formed from the same initial cloud of gas and dust, and they have been observed to have a wide age range, likely being made up of younger or older stars. These star clusters have a density low enough that the individual stars within the open cluster can be observed with a telescope and, at times, even the unaided eye. This is what gives this genre of clusters their "open" appearance[1]. One will often find open clusters to be in the arms of spiral galaxies, with their stars being relatively young. In a steep contrast to globular clusters, open clusters cannot maintain a spherical shape as their structure is inherently unstable and are thus more irregularly proportioned. As such, these stars often disperse as the cluster rotates around the galaxy and are intercepted by the gravitational disruptions of passing cosmic objects.

Figure 1: Open cluster Trumpler 14 NASA, ESA, and J. Maíz Apellániz (Institute of Astrophysics of Andalusia, Spain); Acknowledgment: N. Smith (University of Arizona)[2].

Our research focused on finding the age of globular clusters and considering today's astronomical discoveries. Globular clusters are vastly different from open clusters, most glaringly due to the nature of their composition. Due to the high density of the stars at the center of these spherical clusters, they are hard to discern even with the most powerful telescopes. The large number of stars in a relatively small area leads globular clusters to appear as spherical, though the circumference of these clusters cannot be easily deduced due to the foreground and background cosmological bodies[3].

The results of research led by countless astronomers all conclude that the stars within globular clusters are irrefutably old. Due to changes in luminosity and magnitude as a star ages, the eldest stars tend to be red, while the younger stars tend to be blue. The end of a star's lifespan can be especially violent, resulting in supernovas. Globular clusters are also found in all types of galaxies. Within the perimeter of the Milky Way, globular clusters are found within the *stellar halo,* a spherical population of stars. These stellar halo's surround most disk galaxies and the "cd" class of elliptical galaxies. An estimated one percent of a galaxy's stellar mass resides within this halo[4]. Observing halos in other galaxies is extremely difficult due to its low luminosity. Halo stars residing in the Milky Way are generally old, believed to be an estimated age of 12 gigayears.

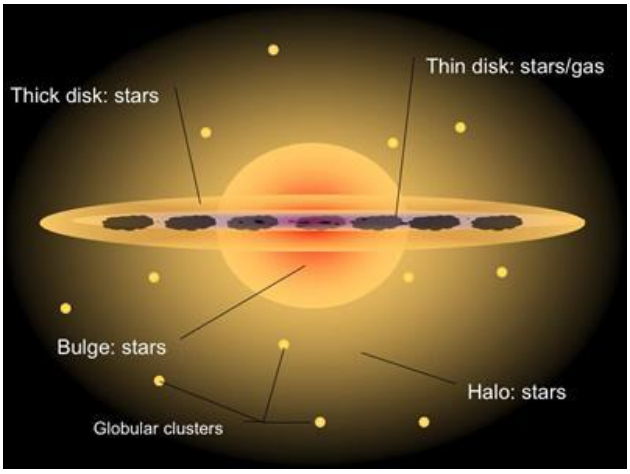

Figure 2: A typical construct of the spiral galaxy has a faint, extended stellar halo [4].

Understanding the age of globular clusters is a key parameter involved in understanding their relationship with galaxy formation and for testing model predictions about the universe[5]. When viewed with the naked eye, globular clusters appear to be faint smudges of light against the darkness of space. However, new telescopes, such as the James-Webb telescope, help resolve these clusters so that they are capable of being imaged and analyzed.

Figure 3: Thousands of stars within globular cluster Terzan 4, part of the constellation Scorpius. The bright, blue stars shown in the center burn hotter and die quickly. The red stars on the outskirts of the cluster burn less hot and are much cooler.[2]

3. Understanding globular clusters

Some globular clusters are found a very large distance away from the galactic center, which is the rotational center, or barycenter, of the Milky Way galaxy. Thus, globular clusters are now focused to be the key object for the study of distant parts of the Milky Way galaxy[6].

Globular Clusters are fossils of the early development of the universe, though not much is known about their origin of creation. It is the gravitational attraction between these stars within globular clusters that allow them to become so long-lived, as they travel in a group together throughout different galaxies. According to the Harvard and Smithsonian Center for Astrophysics, these globular clusters are estimated to have formed around 10 billion years ago, which makes them some of the oldest stars in existence[7].

Since these stars within globular clusters are so old, they are "metal poor" meaning they lack heavy elements that did not exist in the early universe. These elements would be later created by supernovas. Globular clusters are lacking substantially in gas and dust, so the possibility for these clusters to produce new stars is highly unlikely.

One-way researchers can estimate the age of a globular cluster by its metallicity, better defined as the relative amounts of elements heavier than helium. The trend follows that younger clusters have a higher metallicity, while old clusters are "metal-poor", as they were formed before supernovas provided the cosmos with heavier elements to absorb[8]. The stars contained in globular clusters are more condensed than any other place in the galaxy, which leads to the creation of binary systems, including those with compact objects: white dwarfs, neutron stars, and black holes.

B. Structure of Galaxies

1. The Hubble Tuning Fork for Classification of Galaxies

Globular clusters are often an integral part of galaxies. The classification of galaxies based on their structure has evolved throughout the decades. Originating in 1926, the Hubble tuning fork for classification of galaxies has formed the backbone of galaxy classification in recent astronomy. The system categorizes most galaxies as being either elliptical or spiral. Edwin Hubble originally believed that the progression demonstrated the aging process of galaxies. Although this assumption turned out to be incorrect, some of its principles remained, specifically with the nomenclature associated with the system. The terms "early" and "late" are occasionally used to indicate the position of a galaxy on the tuning fork, with "early" indicating that the galaxy is towards the left, and "late" indicating the right. The system has remained a basis for other classification systems through its division between elliptical and spiral galaxies. It begins with a grouping of elliptical galaxies that progresses according to the ellipticity, then branches off into two separate groups: normal spirals and barred spirals[9].

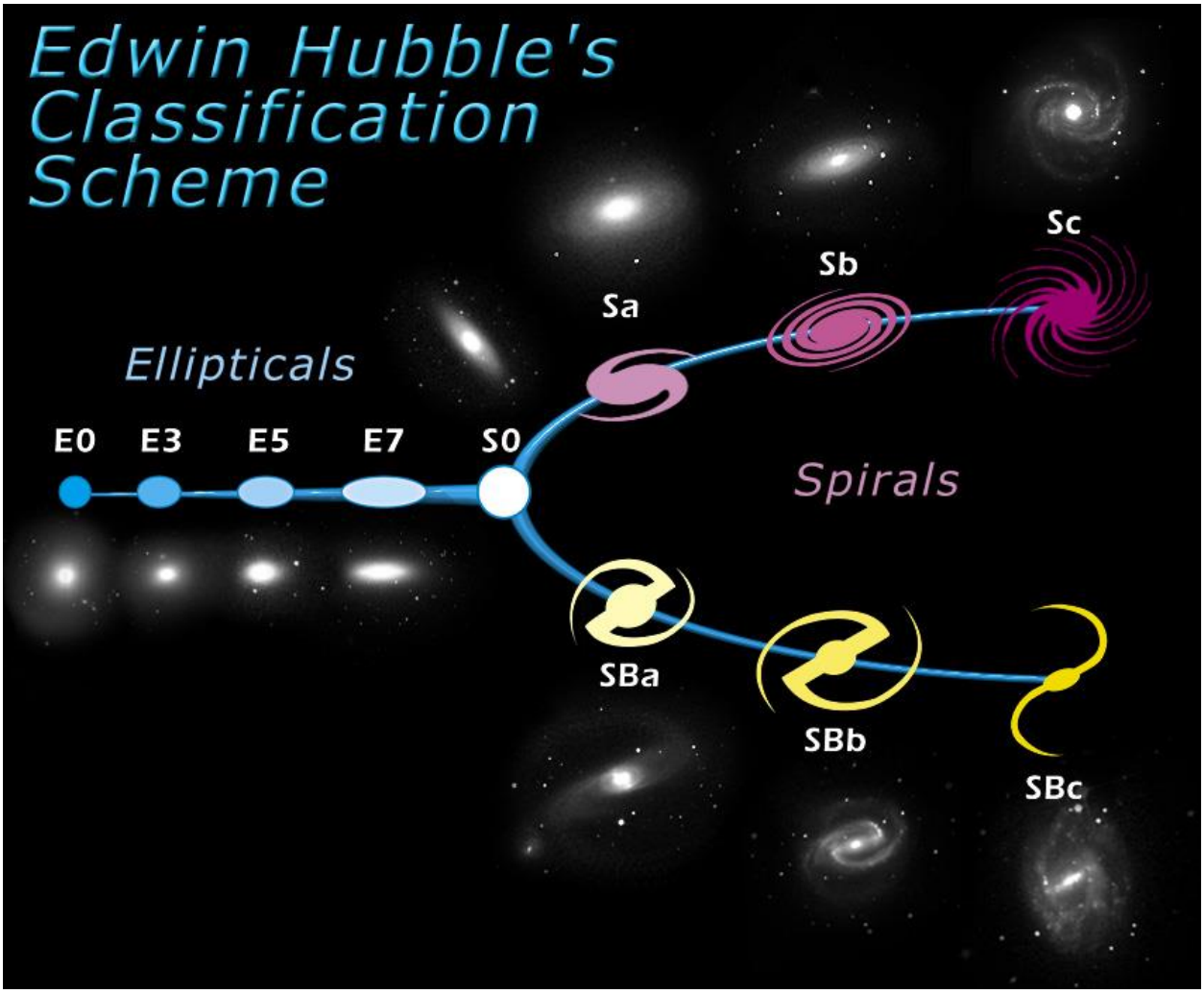

Figure 4: A visualization of Edwin Hubble's Classification Scheme[10].

Spiral galaxies are labeled based on spiral compactness with letters "a-c" in the Hubble tuning fork, with "a" being the most compact. Spiral galaxies are also further classified into two groups: normal spirals and barred spirals. The centers of barred spirals appear to have a bar from which spirals originate, while normal spirals do not contain a bar. A bar is typically a ribbon of stars, gas, and dust that cut across the center of a spiral galaxy. The presence of bars is thought to indicate that a spiral galaxy has reached full maturity. Barred spirals comprise about ⅔ of the spiral group. Normal spirals are indicated with an "S" followed by their compactness level in the labeling system, and barred spirals are indicated with a "SB." Globular clusters are also an integral part of spiral galaxies and are specifically found in arms. These celestial bodies can help suggest the age of a spiral galaxy based on the age of the cluster itself [11].

Elliptical galaxies, which reside on the left side of the tuning fork, are labeled based on an ellipticity from 0-7, with the "0" label indicating that the shape of the galaxy is a near-perfect circle. These galaxies are denoted with an "E" before its ellipticity value. These galaxies contain little gas or dust, and they have very little structure. Because there is not enough gas to form new stars, elliptical galaxies are typically populated with older stars that orbit in random directions. These galaxies are less common than spiral galaxies and are theorized to originate from collisions and mergers with spiral galaxies[11].

Lenticular galaxies are another unique category of galaxies and are indicated with S0 as the transition zone between ellipticals and spirals. These are hybrids between elliptical and spiral galaxies. They contain the central bulge and disk common to spiral galaxies, yet have very little dust and star formation, which is characteristic of elliptical galaxies. It is theorized that lenticular galaxies could be older spirals whose arms have faded, or that they form from mergers between spirals[12].

2. The de Vaucouleurs Classification System

Although the Hubble tuning fork classification system has been useful, it is considered to be an oversimplification, as it doesn't take into account various irregular galaxies. These include galaxies with odd shapes, small dwarf galaxies, and giant elliptical galaxies that reside in the centers of some clusters of galaxies. More modern galaxy classifications take into account the potential irregularities seen throughout the universe. One of the most widely used modern classifications is the de Vaucouleurs Classification system, which is an extension of the Hubble classification system. This system adopted new classifications based on Hubble classifications to denote a transition from well-developed spiral arms to more chaotic structures. This can be seen with the SA and SB structures in the de Vaucouleurs that correspond to Hubble types S and SB, as well as de Vaucouleurs' creation of the "d" and "m" subdivisions within the spiral group. These subgroups extend the way that spiral galaxy compactness is expressed and consider Magellanic Irregulars with the "m" subdivision. De Vaucouleurs also added SAB classifications for oval distortions, which provides a smoother transition between barred and unbarred spirals. Additionally, types "ab," "bc," "cd," and "dm" were adopted to denote smoother transitions from tightly wound to loosely wound spiral structures. Labels (r) and (s) were added to describe the presence and prominence of ring and/or spiral features. Smaller groups that take into account irregular galaxies were also added. Thus, this system broadens the scope of the Hubble tuning fork classification by adding several subgroups that take into account more irregular and unconventional forms of galaxies[12].

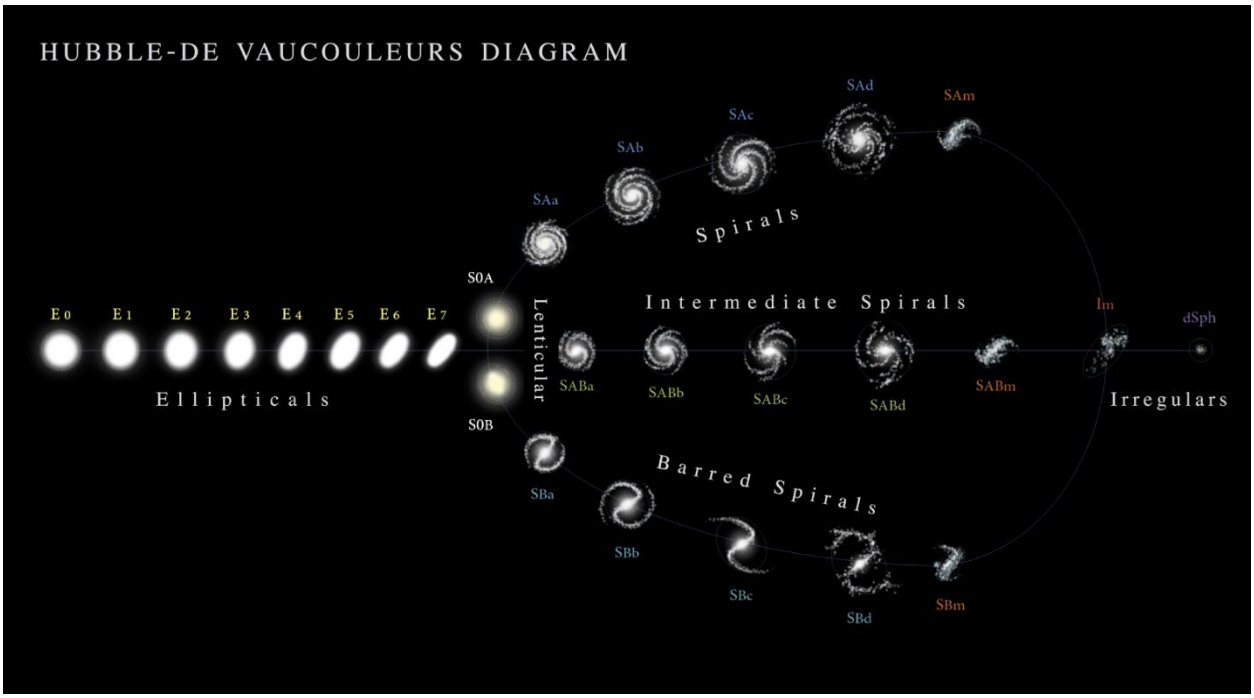

Figure 5: A visualisation of Hubble-De Vaucouleurs Diagram[13].

C. Background on H-R Diagrams

1. Constructing an H-R Diagram

An H-R diagram is one of the most important data analysis tools available to an astronomer. Pioneered in the early 20th century by Ejnar Hertzsprung and Henry Norris Russel, an H-R diagram is a scatter plot that graphs the luminosity of a star against its temperature. Alternatively, it can plot the absolute V magnitude against the (B-V) color of each star[14].

It is known that the hotter a star burns, the more energetic the photons it emits will be. This means that the light of a hotter star will be bluer than that of a relatively cooler star. By extension, when a hotter star is observed, its intensity will be greater in images taken with bluer filters. Similarly, cooler stars would have greater intensities in images with redder filters[14].

Taking the difference in magnitude of a star between its appearance in a bluer filter versus a redder filter, yields a number that relatively ranks the temperature of a star. By general convention this is done with a blue filter and a Visual filter to get the (B-V) color. A visual filter is a type of green filter whose name is derived from the fact that green is the color that the human eye is most perceptive to[14].

When calculating the (B-V) color value, it can be observed that hotter stars have smaller (B-V) color values and cooler stars have larger (B-V) color values. Magnitude is inversely related to the intensity of light, so a hotter star will have more blue light and a smaller B magnitude, making the (B-V) color value smaller. The opposite is true for cooler stars[14].

The V magnitude can be used in place of luminosity precisely because it is the color that the human eye is most sensitive to. It gives a good metric of how bright the star would appear to the human eye, the basis of luminosity[14].

2. Anatomy of an H-R Diagram

Once a collection of stars is plotted on an H-R diagram, a certain trend will become glaringly obvious. Figure 6 shows a general H-R diagram. This line that most stars fall on is called the main sequence. It shows that in general, as the temperature of a star increases, so will its luminosity. It is also observed that most stars in the main sequence differ in mass by no more than one order of magnitude from the sun, therefore the stars in the main sequence can be considered similar in mass[14 15].

There are however some notable exceptions to the main sequence trend. Generally, in the top right of an H-R diagram there is a group of stars which appear to burn too bright for their temperatures. These stars are giants and supergiants, stars near the end of their life which have massively expanded. Additionally, in the bottom left of an H-R diagram are the dwarf stars. These are the leftover cores of stars that have already died. They appear too dim for their measured temperature. The luminosity of a star is proportional to the radius squared and the temperature to the 4th power and the H-R diagram is the visual representation of stellar evolution.

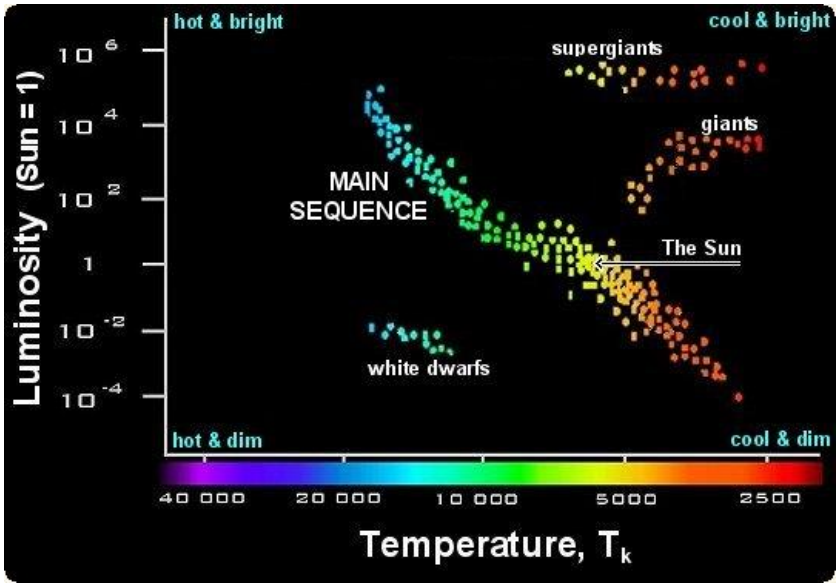

Figure 6: General H-R Diagram with Major Groups Labeled[16].

II. Telescope and Data Collection

A. Allegheny Observatory and PlaneWave Telescope

The telescope used for our research, which can be seen in Figure 7, was a 24-inch PlaneWave telescope, which has a 4K X 4K CCD, a seven-element color wheel, and an f/6.5- and 3974-millimeter focal length. It is the fourth generation Keeler Memorial Telescope and was installed at the historic Allegheny Observatory on August 25, 2022. The current observatory building was built in 1912 and is owned by the University of Pittsburgh.

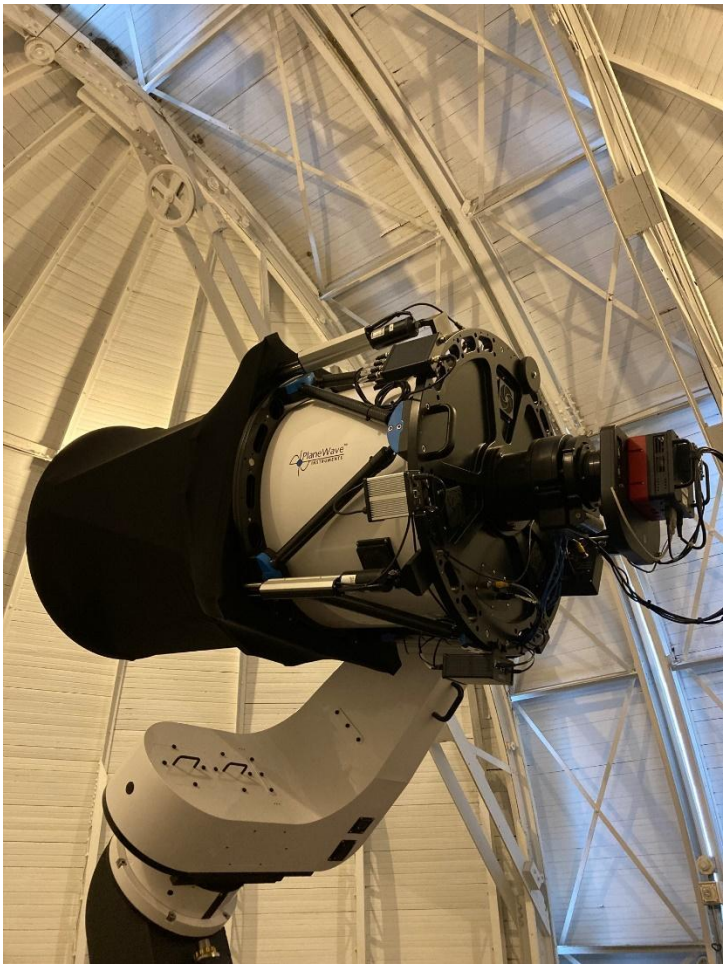

Figure 7: Fourth Generation Keeler Memorial PlaneWave Telescope at the Allegheny Observatory.

As an institution, the observatory was created in 1859, and its first telescope was a 13-inch Fitz refraction telescope. The observatory later obtained a transit telescope, which allowed it to track the positions of the stars to make precise calculations about the time. This information was very valuable to many industries, especially the railroads, and became an important source of income for the observatory[17].

The largest telescope in the observatory is the 30-inch Thaw refraction telescope. For many years, this telescope remained at the cutting edge of observational technology and was the primary instrument of the parallax program, which sought to measure the distances to various stars in the universe to provide some scale for the universe. Parallax involves imaging a star in six-month intervals to observe the star's shift in the sky from opposite sides of the Earth's orbital path. These shifts can be used in a trigonometric calculation to ascertain the star's distance from the Earth[17].

B. Data Collection

To use the PlaneWave telescope, we remotely connected to it via the University of Pittsburgh's secure VPN from Carnegie Mellon University's Doherty Hall. Once connected to the Observatory's computer system,

we were able to operate both the telescope and observatory dome using various software programs, which are referenced in Appendices A – D.

Our observation was conducted over the course of three nights (7/10/23, 7/11/23, and 7/22/23) from around 9:00 pm – 1:00 am. These nights were chosen in particular because there was minimal cloud cover over Pittsburgh. After connecting to the telescope and opening all the required software, we began each night by taking bias frames and flat frames, which are two types of calibration frames that will be explained in a proceeding section. We also focused the telescope using the horizon line.

We then imaged five celestial objects as shown in Table 1. These included the primary focus of our research, the globular cluster M13; the star, Arcturus; the open cluster, M39; the nebula, NGC 6826; and the Veil Nebula. These images were taken in various filters (r', g', Blue, OIII, and Hα) which only allow certain wavelengths of light to be observed as shown in Table 2. Each pixel in the telescope can also be visualized as a "light bucket" which can be overfilled and bled into neighboring pixels, making it necessary to vary exposure lengths to gather the most accurate data possible. Shorter exposures can be used to examine bright stars before their light overflows the buckets in the telescope and longer exposures can be used to examine dimmer stars, which may not have filled the telescope's buckets enough to be observed in shorter exposures.

Table 1: Objects Imaged by our Team with Dates, Filters, Exposure Lengths, and Number of Photos with same Settings

Date	Object Imaged	Filter	Exposure Length (s)	Number of Images with these Settings
7/10/23	Bias	N/A	0	13
	Flat	r'	N/A	13
	Flat	g'	N/A	13
	Arcturus	r'	N/A	2
	Arcturus	g'	N/A	2
	M13	g'	180	3
	M13	r'	180	3
	M39	r'	180	1
	M39	r'	300	1
	M39	g'	120	1
	M39	r'	20	1
	M39	g'	300	1
	M39	g'	20	1
	NGC6826	r'	60	1
	NGC6826	g'	200	1

	NGC6826	Blue	60	1
7/11/23	Bias	N/A	0	11
	Flat	N/A	N/A	24
	M13	g'	10	3
	M13	g'	300	1
	M13	r'	10	3
	M13	r'	300	1
	M13	Blue	15	1
	M13	Blue	30	1
	M13	Blue	120	1
	M39	g'	20	1
	M39	g'	120	1
	M39	g'	300	1
	M39	r'	20	1
	M39	r'	120	1
	M39	g'	300	1
	M39	Blue	20	1
	M39	Blue	120	1
7/22/23	Bias	N/A	0	26
	Flat	OIII	N/A	5
	Flat	g'	N/A	5
	Flat	Hα	N/A	5
	Veil Nebula	OIII	60	3
	Veil Nebula	OIII	180	3
	Veil Nebula	g'	60	3
	Veil Nebula	g'	180	3
	Veil Nebula	Hα	60	3
	Veil Nebula	Hα	180	3

Note: Bias frames can be taken in any filter, but flat frames must be taken in every filter to be used.

Table 2: Wavelengths That Pass Through Each Filter Used[18]

Filter:	Wavelength (nm):
r'	550-750
g'	400-600
Blue	300-400
OIII	499-505
Hα	653-659

It should be noted that the night of 7/10/23 was cut short due to cloudiness, as shown in Figure 8. In addition, on the night of 7/11/23, observation was temporarily interrupted when a loud noise prompted us to take precautionary measures and close the observatory dome for a short period of time.

Figure 8: All-Sky Camera of sky above Allegheny Observatory at 12:39 AM on 7/12/23.

III. Data Reduction

To take pictures with the telescope, we must consider any electronic noise that enters the telescope, internal reflections and any unwanted dust and dirt present on the lens. We do this by taking bias and flat frames. These calibration frames are one of the most important steps when measuring the brightness of stars. When determining the age, there are two main components: magnitude and temperature. To find those, the intensities of the stars in the cluster are required. The intensity can be altered depending on extra

light or dust in the light images, which is why it is crucial to eliminate those errors before determining the age of the cluster.

A. Bias Frames

Bias frames show the electronic noise of the CCD that's unrelated to photons hitting it. This can be very important because without eliminating the bias frames, the final light image can be much brighter than reality. Bias frames are taken without the lens open or pointing at anything, so the picture is in complete darkness. The exposure time for bias frames is near zero, as no outside light is desired. When a bias image is complete, it is observed with counts still in the image. This is exactly what is trying to be removed, since the image was taken in darkness, so there should theoretically be no counts. Typically, several bias images are taken and compiled into one composite image to use for bias subtraction later in the process. In Figure 9 there are counts observed on the left side of the image, which represents electronic noise.

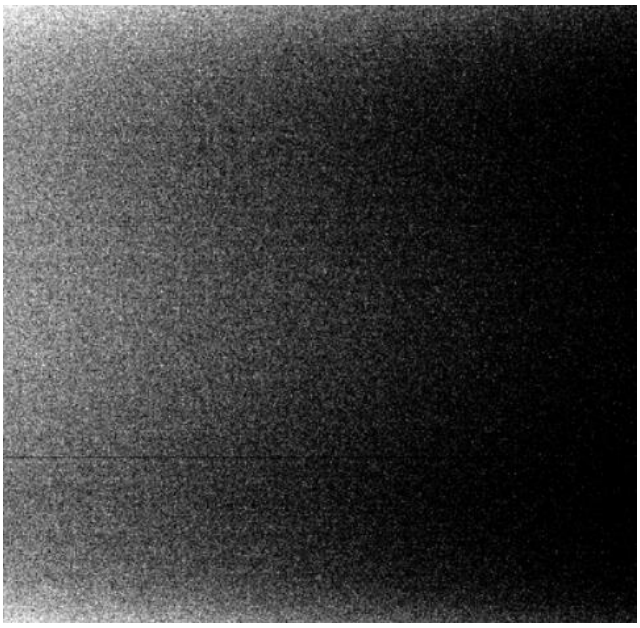

Figure 9: Bias frame taken with PlaneWave Telescope on 7/10/23.

B. Flat Frames

The next step for calibration frames is taking flat frames. Flat frames are the opposite of bias frames, as they are taken of a white board with lots of light coming in. The purpose of flat frames is to eliminate dust and internal reflections in the light images. In the Allegheny Observatory, there is a large square piece of plywood that has been painted white. This is the smooth white field of which the telescope takes pictures. There are two lights shining on the board which bring even more light into the image. For flat frames, the images are taken using the same filters that will be used to take the actual light images of celestial bodies. This is because the light is going through the lens, so the different filters can alter how much light comes in. When the flat frames are complete, it is observed with light in the center and a vignette effect with the black. There are also small donut-like objects visible in the image. This is dust observed on the telescope lens, which also must be removed from the final light images. Similar to the bias, several flat images are taken in each filter being used, which are then compiled into multiple flat composite images for each filter.

The flat composites are used for flat division later in the process. In Figure 10 there are small rings observed in the image, which represent dust.

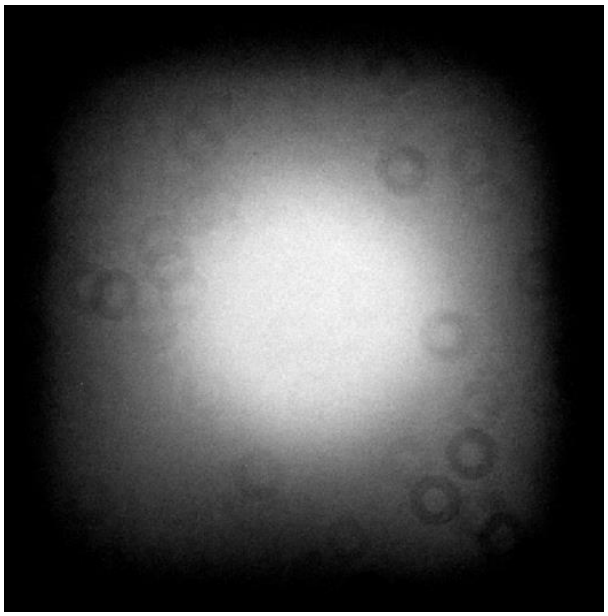

Figure 10: Flat frame taken with PlaneWave Telescope on 7/10/23.

B. Composite Images

Now that all the calibration images were taken, they need to be compiled into composite images using the Data Reduction Facility in AstroImageJ (Appendix A) using a process called “pipelining.” The pipelining process takes all the bias images in one folder and compiles them into one composite image that can be used later. This process repeats for the other calibration frames and for the light image.

The first step of the pipelining process is to create the bias composite. This bias composite will be subtracted from the flat composite and light composite images. Once all bias images are put in one folder, the AstroImageJ Data Reduction Facility selects all of the images in the folder and compiles them into one composite image. Once this image is created, it can be subtracted from the flat images to make a flat composite image.

For the flat composite image, there is still the extra electronic noise, so it needs to be subtracted. Since the bias composite was already created, all that is needed is to enable bias subtraction in the Data Reduction Facility in AstroImageJ. This will remove that extra noise from the composite image that will be created. Similar to the bias composite, all flat images need to be saved to a folder. However, each folder needs to only have one filter in it. There will be several flat composite images made for each filter. Each composite image for the filter will have the bias subtracted from it. Once all of the composites are created, they will later be used for flat division in the light images.

The final step of the pipelining process is to actually create the light images. The end goal with the light images is to be able to get the intensity of the stars to determine the age and to create a three-color image. Since the bias and flat composites were already created, they can now be used for bias subtraction and

flat division for the light composite images. Through the same process as the calibration frames, all of the light frames of one filter need to be saved into a folder. There will be multiple folders for each filter. Once all the folders are made, they can individually be processed through AstroImageJ. Each folder will have the composite bias subtracted and its individual flat composite divided to make it the clearest image possible. Once each folder is processed, there will be individually calibrated images, meaning that the bias is subtracted, and the flat is divided. These images now need to be aligned and stacked together and merged into one single image for each filter. Once this is done there will be light composite images of the celestial object, Figure 11.

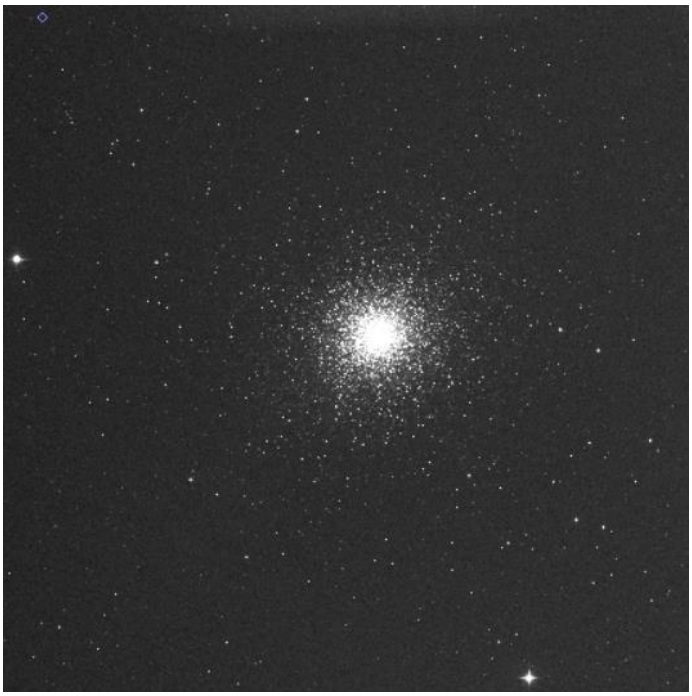

Figure 11: Light composite of M13 from PlaneWave Telescope on 7/10/23 and 7/11/23

D. Photometry

Once the images of an astronomical object are calibrated, there are still a number of calculations that must be done to turn the pictures into usable data. To start this process, images were opened in AstroImageJ to find the intensities of individual stars. Finding the intensity is done using a multistep process called photometry. First, three circles are placed around the star, dividing it into two main regions: the aperture and the annulus as shown in Figure 12. The purpose of these two regions is to compare the photon count coming from the star to the photon count coming from the background, so the amount of light that a star is actually emitting can be determined. After the aperture and annulus are placed, AstroImageJ calculates the total photon count inside the aperture and finds the average photons per pixel of the annulus by counting the photons and dividing them by the area. Next, the photons per pixel of the annulus is multiplied by the area of the aperture, giving the theoretical number of photons in the area of the aperture that would be coming from the background. This amount is subtracted from the total amount of photons in the aperture, leaving only the photons actually coming from the star. AstroImageJ then performs a series of calculations on this value to yield the intensity of the star.

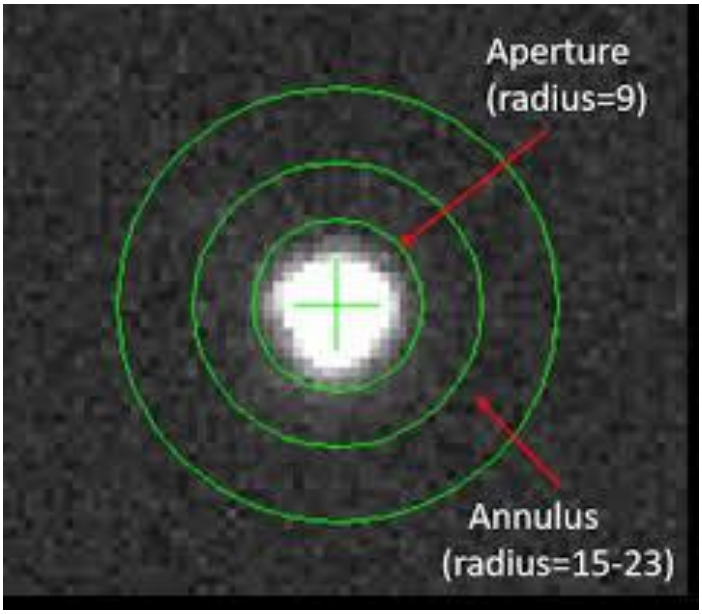

Figure 12: Aperture and annulus during the photometry process[19].

This process was done roughly 900 times to get the intensities of stars in the globular cluster, with all the calculations being done by AstroImageJ software. This data was then entered into Google Sheets and Excel to be organized.

E. Converting to Apparent Magnitude

For this data to be used, it must next be converted from intensities into apparent magnitudes. Intensity is measured with a specific telescope, and is a subjective measurement based on the conditions of the night it is observed. However, the intensity of one star, called a target star, can be compared to the previously known intensity and apparent magnitude of a comparison star, and the apparent magnitude of the target star can be calculated. Because it is calculated in comparison to a star for which the apparent magnitude and intensity are already known, the factors that make the measured intensity of the target star subjective will be accounted for. This is done using the equation

$$m_1 - m_2 = -2.5\left(\frac{f_1}{f_2}\right) \tag{1}$$

where m_1 is the apparent magnitude of the comparison star, m_2 is the magnitude of the target star, and f_1/f_2 is the ratio of their intensities. By using the values for f_1, m_1 (intensity and magnitude of comparison star) and f_2 (intensity of target star), the magnitude of the target star, m_2, can be calculated. This equation was used to calculate the apparent magnitudes for all the stars that were analyzed, using data from SIMBAD (Appendix B) to for the comparison star[20].

F. Converting to Absolute Magnitude

For this project, the data is used in an H-R diagram, which requires the absolute magnitudes of all the stars in a region. The absolute magnitude of a star is the magnitude that it would have if it were viewed ten parsecs away from the sun. Absolute magnitude is necessary because apparent magnitudes don't account for the distance of a star. As a star gets farther away, the light becomes dimmer; without absolute magnitudes, it would be impossible to differentiate between a star that emits a small amount of light but is close to the observer, and a star that emits a large amount of light but is far away from the observer. The absolute magnitude can be calculated by relating the distance of the star and its apparent magnitude in an equation given by

$$m - M = 5(d) - 5 \quad (2)$$

where m is the apparent magnitude, M is the absolute magnitude, and d is the distance of the star.

Once these calculations were done, there was a lack of particularly dim stars from the data taken with the telescope, so it was supplemented with data from SIMBAD.

IV. H-R Diagrams for Globular Clusters

There are some unique features in H-R diagrams for globular clusters, an example of which can be seen in Figure 13. Most obvious is the significant deviation from the main sequence as temperature increases. This phenomenon occurs because all the stars in a globular cluster were born at around the same time, but they do not all burn at the same temperature. The hotter a star burns, the quicker it will use up its fuel, meaning a hotter star's lifespan is shorter than its cooler relatives. The hotter stars will enter their giant phase earlier, and that is why this *turn-off point* can be observed in the H-R diagram[21].

As it turns out, this phenomenon is one of the things that makes globular clusters so interesting to study. By measuring the absolute V magnitude where the turn-off point occurs, it can be found what type of stars have most recently entered their giant phase, and an Isochrone chart (shown in Figure 14) can be used to find which points correspond to which ages[21].

In general, globular clusters tend to be some of the oldest stellar structures in the universe. For that reason, it is also common for the H-R diagram of a globular cluster to include a *horizontal branch*. These are stars that are so old that they are burning helium instead of hydrogen, causing them to deviate from the main sequence[21].

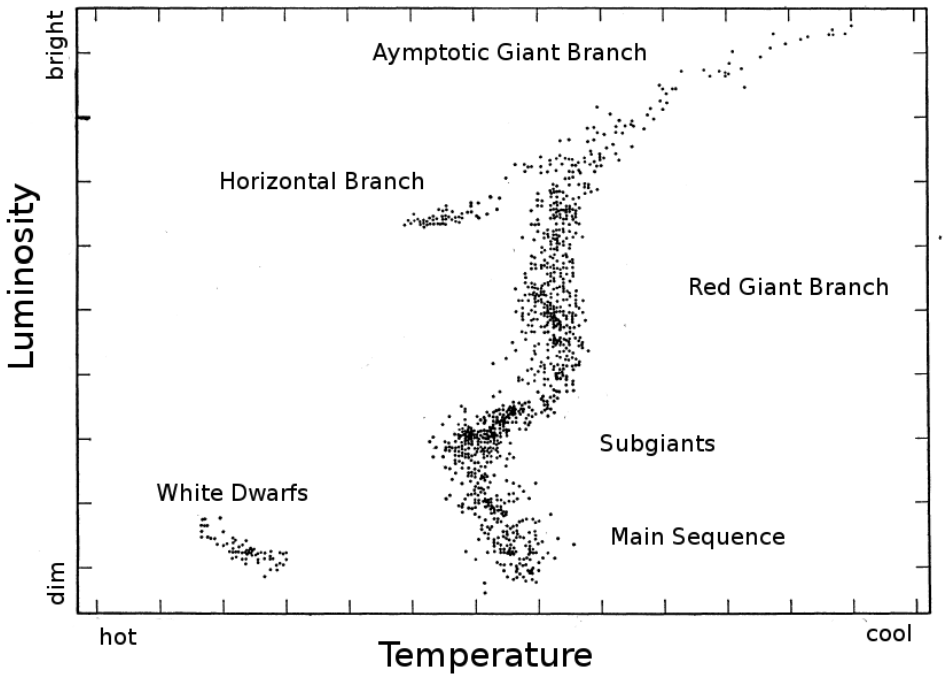

Figure 13: General H-R Diagram for Globular Clusters [22].

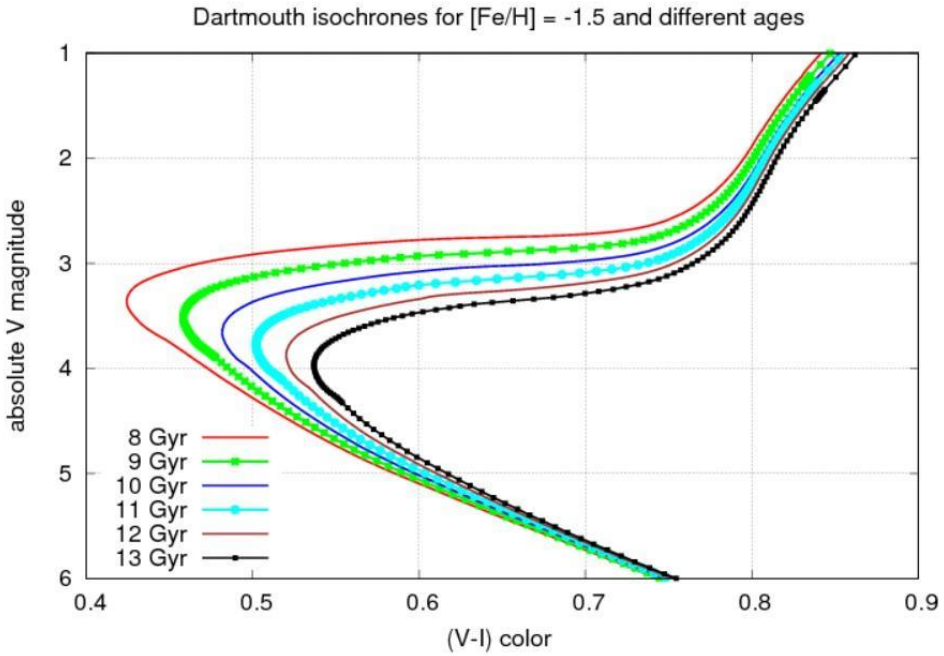

Figure 14: Isochrone Chart

V. Our H-R Diagram

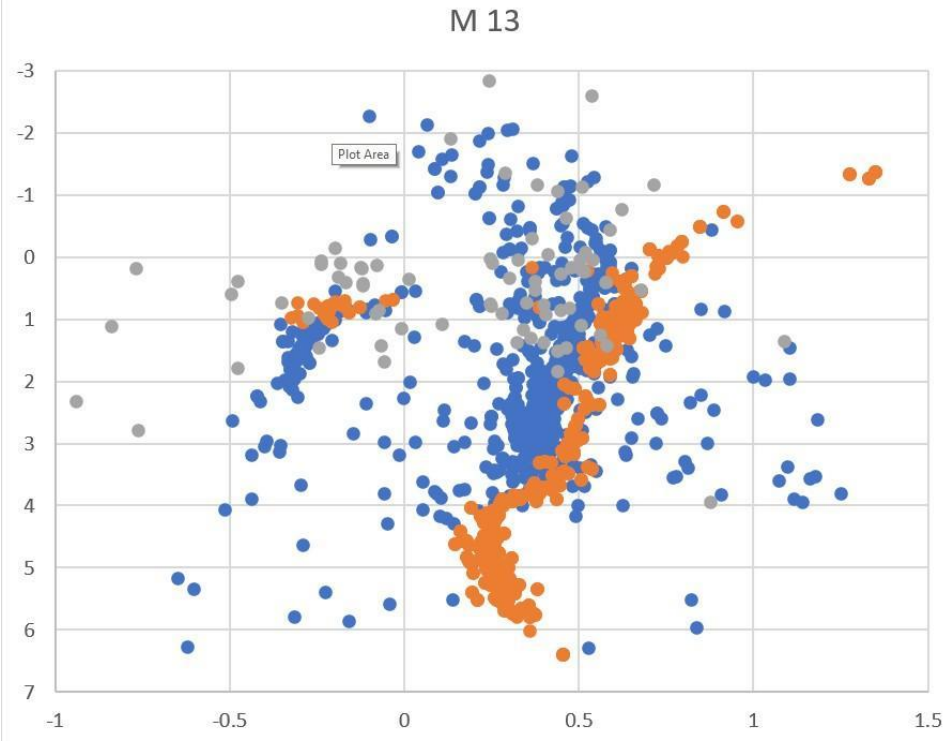

Figure 15: H-R diagram of M13.

Using the data that was collected from the images of M13, an H-R diagram was constructed to determine the age of the globular cluster. The diagram utilized data from 300-second and 10-second-long exposures and used roughly 900 stars altogether. It was supplemented by data from SIMBAD, an astronomical database with basic information about objects outside the solar system. This was done to better define the main sequence of the diagram, especially the fainter stars. Because the M13 globular cluster is so old, its turnoff point is defined mostly by older, fainter stars that were not captured in the images we took. This is another reason why the data used in the H-R diagram was supplemented with SIMBAD.

On the diagram, the y-axis represents the absolute g' magnitude, while the x-axis represents temperature. One notable aspect of the diagram is the cluster of stars on the upper left side, which is M13's *horizontal branch*. The presence of this branch indicates the old age of M13 and helps support the greater conclusion regarding the age of the cluster that was drawn from the diagram.

A. Interpreting our H-R Diagram

The H-R diagram above reveals a significant amount of information about the age of the M13 globular cluster. The approximate age can be determined by correlating the absolute g' value of the turnoff point to an age using an isochrone chart. To do this, the turnoff point was first determined to be at an absolute g' magnitude of roughly 4.5. This value was then translated into an absolute V magnitude because the isochrone chart used an absolute V magnitude scale. To perform this translation, a series of calculations were performed that culminated in subtracting the absolute g' magnitude by a value of 1.1. This produced an absolute V magnitude of 3.4. This value was then compared to an isochrone chart, which correlates absolute V magnitude and metallicity, or the relative ratio of the quantity of other metals and materials to hydrogen, to determine the age of a celestial object.

Figure 14 demonstrates a series of ages for a metallicity of -1.5 depending on an absolute V magnitude. The metallicity of a celestial object does not change after its birth. The metallicity of M13 has been previously determined to be -1.5. The above chart demonstrates several different potential ages and their corresponding curves. The absolute V magnitude of M13 was determined to be 3.4; the peak of the 9 gigayear curve matches this value most closely. Therefore, M13 was determined to be 9 gigayears old. This compares well with the accepted age of 11 gigayears.

B. Considering Potential Errors

Potential errors and inaccuracies that occurred during this process should be considered. One item that did not impact the integrity of our data but could have been helpful in pinpointing the age of M13, would have been to add error bars on our data. We also did not get an adequate sampling of dim stars, which was impactful because the turnoff point of M13 was mainly defined by older, dimmer stars. Another potential source of error could have been that we did not remove any foreground or background objects, which include several stars and galaxies. The light of these objects had the potential to compromise our data. We also did not correct for any gravitational lensing or redshift effects, but these topics will be discussed later in this paper.

VI. Other Imagery

When the images are processed, there will be multiple composite images with different filters. These filters can be used to create three color images. Each composite image is slightly different depending on how much light came through the filter. This means that when the images overlap, there will be some layers that are different and some that are the same. When colors are assigned to the different layers, multiple colors come through and a beautiful image is created.

A. Using FitsLiberator

After creating the composite images, they are saved as FITS (Flexible Image Transport System) File. These composite images can then be uploaded into a program called FitsLiberator (Appendix C). This program allows grayscale scaling to be nonlinear and brings out fine details in order to get the clearest and sharpest image possible. This process gets repeated for all light composites with different filters.

Using PhotoPea, these images can be layered on top of each other. Each layer will get a different color assigned to it based on its wavelength. For example, the shorter wavelengths (400-550 nm) will be blue, the medium wavelengths (550-700 nm) will be green, and the longest wavelengths (700-900 nm) will be red. When all the layers have a different color, a beautiful three-color image will be created. A few extra steps to make the image clearer would be to add curves into the layer. These curves will change the amount of color shown on the screen, so there can be more or less of one color to make the image clearer or brighter.

B. Messier 13 Three-Color Image

For M13, our color image was very purple. This is because our main images were from blue and red wavelengths. Our third filter was more of a supplemental filter, so the major colors are still blue and red. We applied the same imaging process as described above to create our three-color image of M13 as shown in Figure 15.

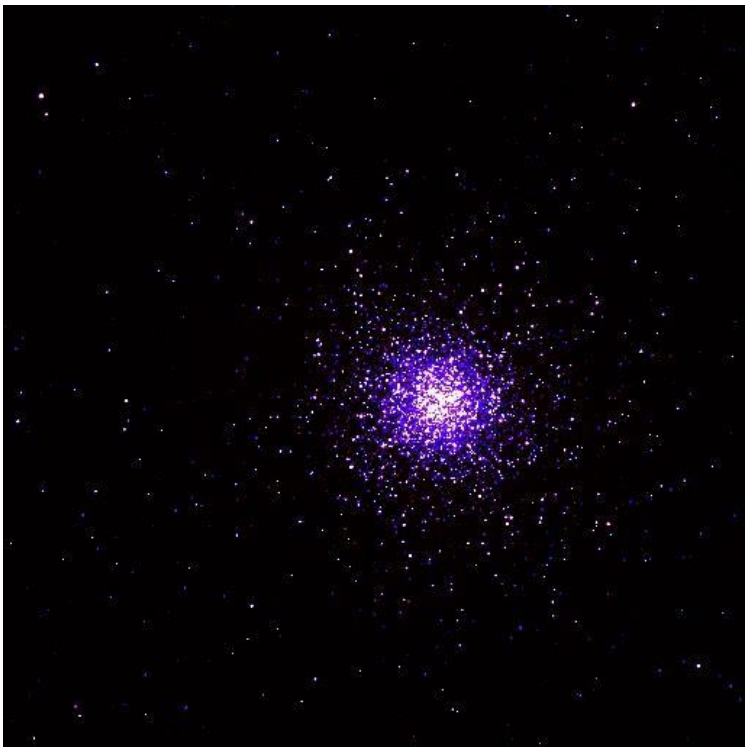

Figure 15: Three-color image of Messier 13 globular cluster.

C. Veil Nebula Three-Color-Image

On a separate night, we took images of the Veil Nebula. We did not use these images to determine the physical properties of the nebula but to generate our own three-color image of a nebula in space. The three filters that we used for this process were g', OIII, and H-Alpha. The Veil Nebula is an emission nebula and is very bright in the emission lines of Hydrogen and doubly ionized Oxygen. We still went through the pipelining process with bias and flat frames, and then created our light images in the three different filters. When we generated our three-color image, the nebula was mainly green and red. This was because the OIII and H-Alpha filters let in a smaller amount of light, so the nebula showed up very bright. The g' filter lets in more light, but that also means that the images are less clear. As a result, the g' filter left mainly stars in the image and didn't show much of the nebula. When layering the images all together, we were able to get a very clear image of the Veil Nebula, with predominantly red and green colors as shown in Figure 16.

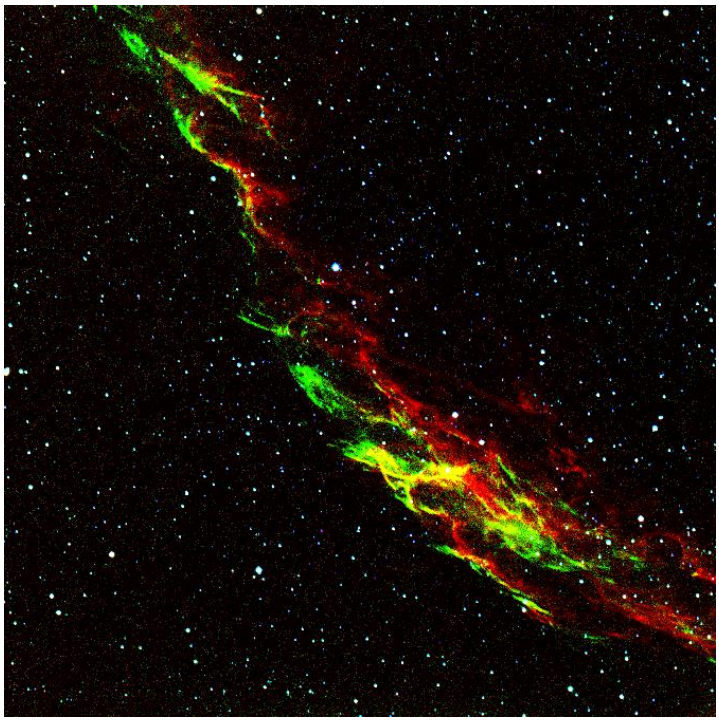

Figure 16: Three-Color-Image of the Veil Nebula taken with the PlaneWave Telescope on 7/22/23

D. Hubble Legacy Archive

Another project that we worked on was taking images from the Hubble Legacy Archive (Appendix D) and making three color images out of them. The Hubble archive has gray-scale images of several nebulas, galaxies, globular clusters, and other galactic structures. These gray-scale images have different filters for each image that we can download and make our own images out of them. We used the same software, FitsLiberator, to adjust the gray-scale images from the archive. Then we put all of the images with the different filters into PhotoPea to make our three-color images. We did this for several nebulas including the Eagle Nebula, Orion's Nebula, Lagoon Nebula, Omega Nebula, and ESO Planetary Nebula as shown in Figure 17.

Figure 17: Three Color Images Created Using Grayscale Images from Hubble Legacy Archive Going clockwise from top left: Eagle Nebula, Lagoon Nebula, Omega Nebula, ESO Planetary Nebula, Orion's Nebula

VII. Redshift

A. Defining Redshift

'Red shift' is an important calculation used by astronomers that helps compare the distance of faraway galaxies, as well as offering insight to the chemical composition of distant celestial objects[23]. There are three kinds of 'redshift': astronomical, gravitational, and doppler. This experiment only requires the use of astronomical redshift and doppler redshift, as gravitational red shift does not pertain to the scope of the experiment's research goals. The idea of redshift is better understood using the context of what some might have heard of: the Doppler effect. Doppler effect transpires when a source of sound moves relative to an observer. It was discovered and named after Christian Andreas Doppler, an Austrian mathematician who discovered the frequency of sound wave changes[24]. Numerous examples of the Doppler effect include the changing of pitch of police and ambulance sirens, or train whistles and racing car engines as they pass by.

B. Doppler Redshift

Considering the fact that light behaves similarly to a wave, the light from a luminous celestial object (in this case globular clusters) undergoes a Doppler-like shift if the source is moving relative to the observer's perspective. Edwin Hubble, the American astronomer who discovered the universe is expanding in 1929, has motivated astronomers to continue their study of redshifting by assuming that *most* other galaxies are

moving away from Earth. The wavelength of light emitted by these galaxies becomes stretched the farther it moves away from the observer, causing it to appear as 'redshifted'.

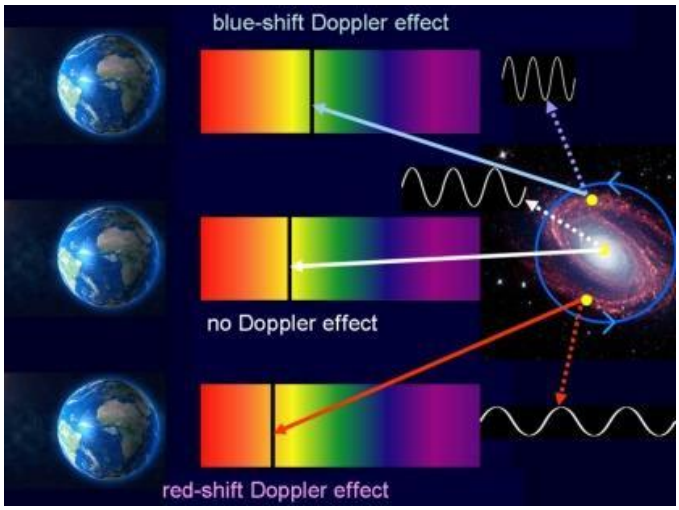

Figure 18: As a celestial object emitting light moves closer to the observer, the frequency of the wavelength grows compressed, and will appear blue. However, if the object were to be moving away from the observer, the wavelength would stretch, and it would appear red to the human eye [25].

The red shift of a specific globular cluster can be easily measured by comparing its respective spectrum with a reference laboratory spectrum. At well-known wavelengths, absorption lines can be used as a reliable indicator to determine the redshift of the receding astronomical objects by measuring the location of these lines in astronomical spectra.

When the velocity of the astronomical object is comparably small to that of the speed at which its light waves propagate, the magnitude of either the redshift or the blueshift is referred to as variable 'z' and is given by

$$z = \frac{\Delta\lambda}{\lambda_{rest}} = \frac{\lambda_{obs} - \lambda_{rest}}{\lambda_{rest}} = \frac{v}{c} \quad (3)$$

where $\Delta\lambda$ is the change in wavelength of the light, λ_{rest} is the wavelength of the light if the object was stationary, λ_{obs} is the observed wavelength of the light, v is the velocity of the moving object, and c is the speed of light in a vacuum.

C. Absorption Lines & Spectra

Astronomers are then able to observe how redshift and blueshift transpire over time by using a high-resolution prism-like instrument also known as a spectrograph. The spectrograph separates the incoming wavelengths of light into an array of colors, also known as the spectra.

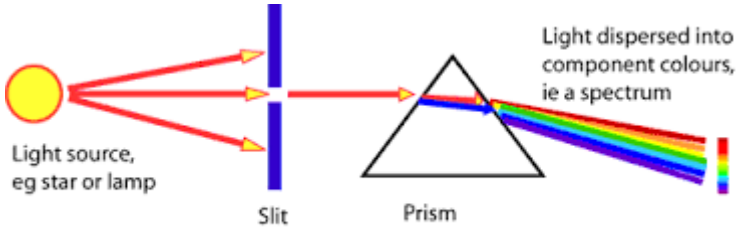

Figure 19: The process of using a spectrograph
Source: Australia Telescope National Facility[26].

Within every star, there are atoms that absorb light at specific wavelengths, and these absorptions appear as dark lines in the different colors of the star's spectrum, better known as spectra. Researchers use the shifts in these lines as convenient markers to measure the size of a Doppler shift.

Knowing the specific frequencies of Hydrogen lines, astronomers study light emitted by these stars. You can substitute Hydrogen with different elements or molecules to get completely different distinct patterns of absorption lines, also known as the distinct absorption fingerprints. From these distinct absorption fingerprints, astronomers are able to discover the chemical makeup of stars and galaxies[26].

C. Relativistic Doppler Effect

A more mathematical approach to the Doppler effect leads one to understand the special relativity behind 'The Relativistic Doppler Effect' equation. This formula begins with the general understanding that waves of any sort- whether sound or light- that are emitted at some frequency by a moving object are perceived differently by a stationary observer.

When both the source of the wave as well as the observer are both stationary, the observer would 'see' waves of frequency, **(ν)** or wavelength, **(λ).**

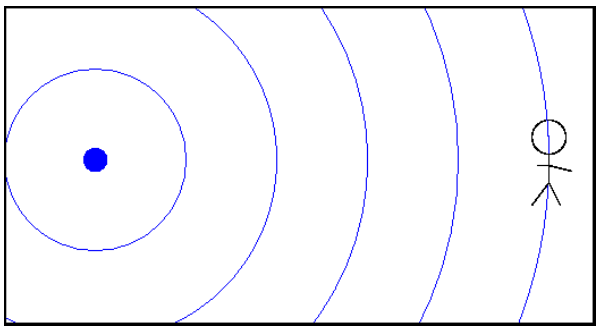

Figure 20: A stationary source of wavelength (left) and a stationary observer (right) as the waves emitted by the stationary source reaches the observer [27].

However, if the source was moving towards the observer, then the frequency which is perceived by the observer (**ν') would** be faster than the actual emitted frequency, thus the understood wavelength from the perspective of the observer (**λ') is** shorter than the emitted wavelength.

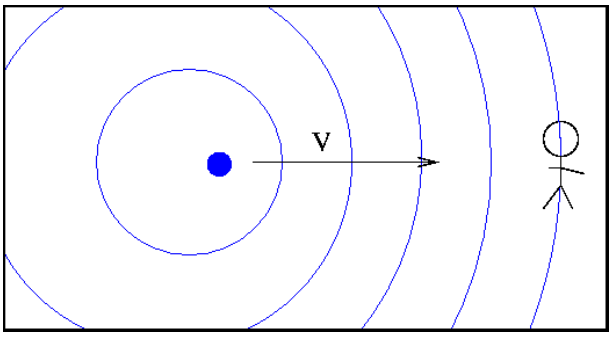

Figure 21: This source of wavelength (left) as it moves towards the observer (still stationary) at a certain velocity (v') would cause the frequency to be perceived as higher, while the wavelength would be shorter[27].

Astrophysicists can connect the emitted and observed frequencies and wavelengths of Doppler shifted light by equations given by

$$f' = \frac{f}{1 \mp \frac{v}{c}} \tag{4}$$

and

$$\lambda' = \lambda\left(1 \mp \frac{v}{c}\right) \tag{5}$$

where f' and λ' are the frequency and wavelength respectively perceived by the observer, f and λ are the frequency and wavelength respectively emitted from the object, v is the velocity of the object, and c is the speed of light in a vacuum.

It should be noted that the shift in wavelength for a moving source moving *towards* the observer is directly inverse to the shift for a source moving *away* from the observer.

By using the postulates of Einstein's Theory of Special Relativity, astrophysicists can derive a different relationship between frequency and motion[5]. A simple way to understand it is to note that the time on a moving source runs slow by factor of 'γ' so that it appears to a stationary observer that it would take a bit longer to create each wave crest. Therefore, the rate at which new wave crests appear (frequency) is slowed down by γ. The equation is given by

$$v' = \frac{v}{1 \mp \frac{v}{c}} \frac{1}{\gamma} \tag{6}$$

which, after doing some algebra, can be simplified to

$$v' = v \frac{\sqrt{1 - \frac{v}{c}}}{\sqrt{1 + \frac{v}{c}}} \tag{7}$$

where velocity is negative, the source and object are approaching each other. Where the velocity is positive, the source and object are retreating from each other. Using this equation, astronomers can now measure the speed at which stars are either approaching or receding from the observer.

E. Astronomical Redshift

The red shifts observed in distant objects are not entirely due to Doppler redshifting, but are also affected due to the expansion of the universe. While Doppler redshifts stem from the relative motion of the source of frequency and the observer through space, astronomical redshifts take into account the expansion of space itself[6]. This means that although two astronomical bodies can be stationary in space, they will still be subject to astronomical red shifting due to the rate at which the universe is growing.

In the early 20th century, the astronomer Edwin Hubble observed that the spectra of distant galaxies were significantly redshifted. Edwin Hubble determined that this drastic shift in the spectrum is reliant on velocity in which these galaxies were receding, which was also proportional to how far they are relative to the observer.

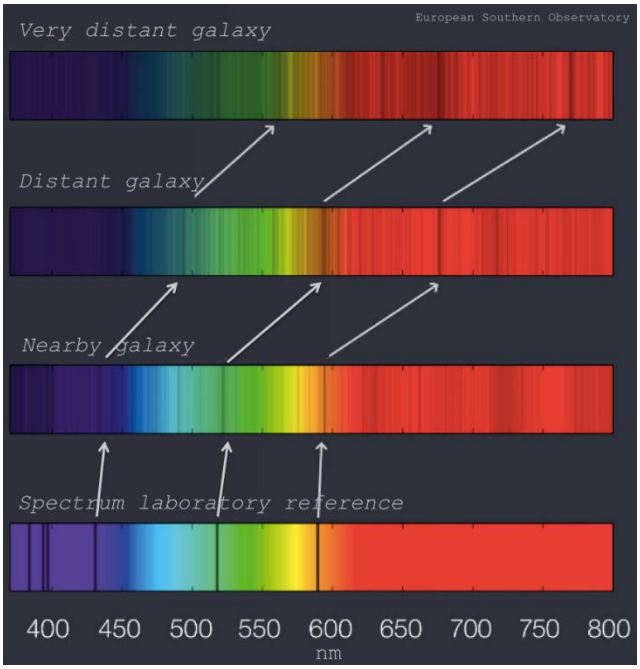

Figure 21: This shows the difference in spectra among nearby galaxies, distant galaxies, and very distant galaxies. As previously stated by Hubble's discovery, the farther the galaxy is relative to the observer, the farther it is redshifted[28].

Hubble's conclusion that the velocity in which the galaxies are receding from the observer is equal to the distance is mathematically shown in Hubble's Law.

F. Hubble's Law

Hubble's law, as an example, can be represented graphically by creating a plot of multiple different observed galaxies. The x-axis of the chart depicts the distance, "d", of each galaxy- typically in megaparsecs. On the y-axis, astronomers plot the velocity, "v", at which the celestial body is receding relative to the observer. This is usually measured in kilometers per second, km/s.

The slope of the line created is called, 'H_0', pronounced H-naught, also known as the Hubble constant which has a value of roughly 68.8 km/sMpc.

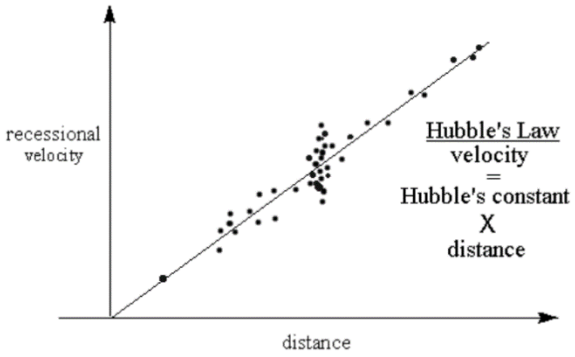

Figure 22: This shows Hubble's law depicted graphically as it created a plot of each observed galaxy using the velocity in which it is receding from the observer (recessional velocity) over the distance that it is relative to the observer (measured in megaparsecs)[29].

From this law, he, as well as a few other astronomers, were able to conclude several important facts pertaining to the nature of this Universe. These conclusions stem from the claim that all galaxies appear to be receding from a specific point in space. This stems from the fact that the entire universe is constantly expanding; therefore 3-D space-time itself is stretching apart. Regardless of the vantage point, all galaxies appear to be moving away[30]. Hubble deduced that the farther away the galaxy is, the higher velocity in which it is receding. Additionally, the rate of expansion of the Universe is steadily growing faster than how it used to when the Universe was young.

This expansion of space-time is more simply depicted using the analogy of baking a blueberry muffin. The batter will represent the Universe and the blueberries are all which reside within it. Although the blueberries themselves remain stationary in their own perspective, as the batter continues to bake, it causes the blueberries to move as well. The blueberries furthest from each other move away the quickest.

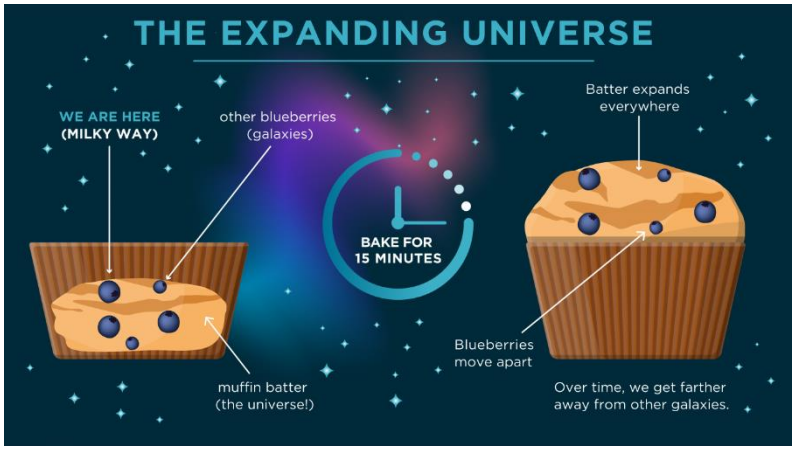

Figure 23: A drawn example of the blueberry muffin analogy used to explain the expansion of the universe [29].

The first conclusion made by Hubble and a few other astronomers was that if the Universe is always moving apart, then if one were to rewind to the early Universe, everything would be compact into one small point. This single hot point then rapidly expanded outward: the moment of the Big Bang.

If astronomers were to look at galaxies of ranging distances and observe how fast they are receding due to the expansion of space-time, they would determine that there was a varying rate for the expansion of the universe[30]. Regardless of the varying speed, astronomers can then work backwards to further understand when the movement began. From Hubble's observations, astronomers can confidently conclude how long ago the Big Bang occurred, and therefore estimate the age of the universe.

VIII. Gravitational Lensing

Gravitational lensing is a phenomenon that is often observed when looking into deep space. It occurs when a massive celestial body causes a curvature of spacetime large enough to bend light. This can occur with any massive enough object, including globular clusters such as M13. The body causing the light to bend is referred to as the gravitational lens. It was first proven during the solar eclipse of 1919, when astronomers witnessed the sun bending the light of background stars by the amount predicted by Albert Einstein.

The phenomena works in conjunction with Einstein's theory of relativity. This theory states that space and time are fused together in a body called spacetime that makes up the "fabric" of the universe. One of the major ideas of this theory is that massive objects distort spacetime in a manner that can impact the path of anything traveling in the impacted region, including light itself.

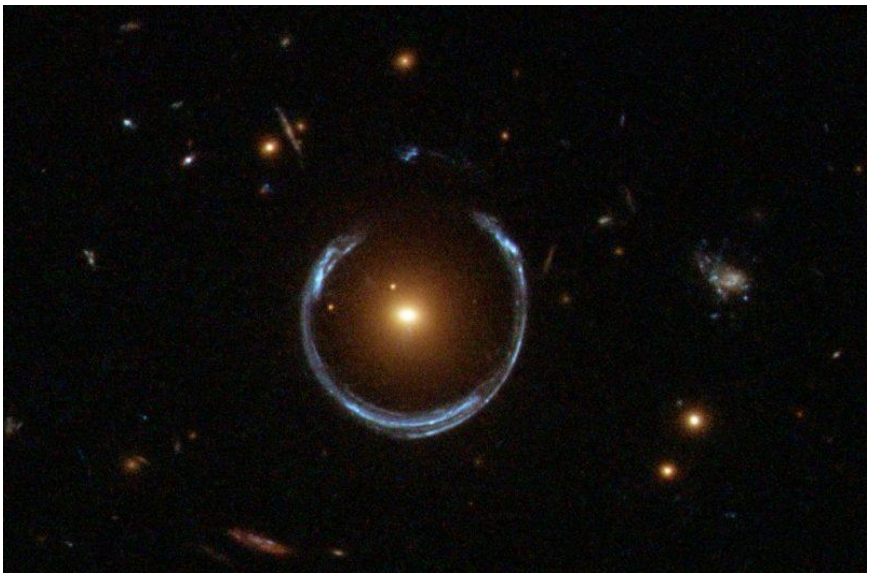

Figure 24: This image, taken by the Hubble Space Telescope's Wide Field Camera 3, depicts a luminous red galaxy with a strong gravitational impact that warps the light of a more-distant blue galaxy[31].

Gravitational lensing is useful because it helps astronomers detect and understand the presence of dark matter in the foreground of galaxies. Although dark matter makes up as much as 85% of the total mass in the universe, it emits no light, and therefore is challenging to detect. However, astronomers can study gravitational lensing to discern the location of dark matter based on its impact on the light around it. In this way, gravitational lensing contributes to humanity's understanding of the universe[31].

IX. Conclusion

Globular clusters are a very important and interesting part of the universe. They are compact, spherical groups that consist of millions of stars, and move through the universe as a whole. Because the stars within globular clusters are so old, there are a number of insights that can be gained only from these clusters. While their origins are not fully understood, they provide a way to learn more about the distribution of dark matter, the age and history of the universe, and different features of galaxies.

In this project, the age of the globular cluster M13 was determined through a long process involving gathering data with a telescope, processing the data, and plotting an H-R diagram that was then compared to an Isochrone chart. Images with varying exposure lengths and different filters were taken with a 24" PlaneWave telescope, which were then calibrated using bias and flat frames that were also taken on the telescope. AstroImageJ software was used to find the intensities of individual stars in the cluster through photometry. This data was then converted from intensities to apparent magnitudes, then to absolute magnitudes. The absolute magnitudes were then plotted on the H-R diagram. The H-R diagram plots the absolute magnitude on the y-axis and the value of the blue light minus visual (green) light, which represents the temperature. This was then compared to an Isochrone chart, which shows how the turnoff point on the H-R diagram indicates the age of the cluster.

Through this comparison, M13 is estimated to be 9 gigayears old. The effect of gravitational lensing and redshift is discussed, as it pertains to potential errors in the data and results. After the data is used for determining the age of the cluster, the pictures taken with the telescope were then colored and layered to create 3-color images of various celestial objects. Along with these pictures, other 3-color images were created using grayscale images from the Hubble Legacy Archive. In conclusion, globular clusters are some of the most interesting celestial objects to study as they give insights into the nature of the universe as a whole.

X. Appendix

A. AstroImageJ

AstroImageJ is ImageJ with astronomy plugins and macros installed. It includes tools based on the Göttingen ImageJ astronomical resources with additions we find useful.

B. Simbad

The SIMBAD astronomical database provides basic data, cross-identifications, bibliography, and measurements for astronomical objects outside the solar system. SIMBAD can be queried by object name, coordinates, and various criteria.

C. FitsLiberator

The ESA/ESO/NASA FITS Liberator is a free software program for processing and editing astronomical science data in the FITS format to reproduce images of the universe.

D. Hubble Legacy Archive

The Hubble Legacy Archive (HLA) is designed to optimize science from the Hubble Space Telescope by providing online, enhanced Hubble products and advanced browsing capabilities. The HLA is a joint project of the Space Telescope Science Institute (STScI), the Space Telescope European Coordinating Facility (ST-ECF), and the Canadian Astronomy Data Centre (CADC)

XI. References

[1]Information@eso.org. “Open Cluster.” *ESA/Hubble | ESA/Hubble*, esahubble.org/wordbank/open-cluster/. Accessed 3 Aug. 2023.

[2]Gianopoulos, Andrea. “Discoveries - Hubble’s Star Clusters.” *NASA*, 17 Nov. 2022, www.nasa.gov/content/discoveries-hubbles-star-clusters.

[3]“Halo: Cosmos.” *Halo | COSMOS*, astronomy.swin.edu.au/cosmos/h/halo. Accessed 3 Aug. 2023.

[4]*Globular Cluster Systems - California Institute of Technology*, ned.ipac.caltech.edu/level5/Ashman/Ashman1.html. Accessed 4 Aug. 2023.

[5]Mohon, Lee. “Galactic Center.” *NASA*, 22 July 2019, www.nasa.gov/mission_pages/chandra/images/galactic-center.html.

[6]*Globular Cluster Formation and Evolution in the Context of Cosmological ...*, royalsocietypublishing.org/doi/10.1098/rspa.2017.0616. Accessed 3 Aug. 2023.

[7]"Star Clusters." *Star Clusters | Center for Astrophysics*, pweb.cfa.harvard.edu/research/topic/star-clusters. Accessed 3 Aug. 2023.

[8]Trevor. "What Is a Globular Cluster?: Pictures, Facts, & Best Ones to Observe." *AstroBackyard*, 26 Oct. 2022, astrobackyard.com/globular-clusters/.

[9]Information@eso.org. "The Hubble Tuning Fork - Classification of Galaxies." w*ww.Spacetelescope.org*,esahubble.org/images/heic9902o/. Accessed 4 Aug. 2023.

[10]*Astronomy 505*, astronomy.nmsu.edu/nicole/teaching/ASTR505/lectures/lecture27/slide01.html. Accessed 3 Aug. 2023.

[11]*Spiral Structure in Galaxies: The Classification of Galaxies - IOPscience*, iopscience.iop.org/chapter/978-1-6817-4609-8/bk978-1-6817-4609-8ch2.pdf. Accessed 4 Aug. 2023.

[12]"Types of Galaxies." *NASA*, 10 Apr. 2023, universe.nasa.gov/galaxies/types/.

[13]*Grard de Vaucouleurs' Atlas of Galaxies*, cseligman.com/text/devaucouleurs.htm. Accessed 3 Aug. 2023.

[14]*The Hertzsprung-Russell (HR) Diagram*, spiff.rit.edu/classes/phys230/lectures/hr/hr.html. Accessed 3 Aug. 2023.

[15]Sloan Digital Sky Survey (SDSS) Filters. - Researchgate, www.researchgate.net/figure/Sloan-Digital-Sky-Survey-SDSS-filters_fig5_235663628. Accessed 4 Aug. 2023.

[16]"Hertzsprung Russell Diagram." *AstroPages | HR Diagram | Western Washington University*,

[17]*History of Allegheny Observatory*, sites.pitt.edu/~aobsvtry/history.html. Accessed 3 Aug. 2023.

[18]"Mass, Luminosity, and the HR Diagram." Mass and Luminosity, pages.uoregon.edu/soper/Stars/hrmass.html. Accessed 4 Aug. 2023.

[19]Conti, Dennis M. *Exoplanet Observing*, astrodennis.com/Guide.pdf. Accessed 4 Aug. 2023.

[20]"17.1 the Brightness of Stars - Astronomy." *OpenStax*, openstax.org/books/astronomy/pages/17-1-the-brightness-of-stars. Accessed 3 Aug. 2023.

[21]*Durham E-Theses Globular Cluster Systems and Their Implications Of ...*, etheses.dur.ac.uk/2427/1/2427_438.pdf. Accessed 4 Aug. 2023.

[22]"The Life Cycle of Stars." *The Life Cycle of Stars | Max Planck Institut Für Sonnensystemforschung*, www.mps.mpg.de/de/sage/life-cycle-stars. Accessed 3 Aug. 2023.

[23]"What Do Redshifts Tell Astronomers." *EarthSky*, 2 Jan. 2022, earthsky.org/astronomy-essentials/what-is-a-redshift/.

[24]"What Is 'Red Shift'?" *ESA*, www.esa.int/Science_Exploration/Space_Science/What_is_red_shift. Accessed 3 Aug. 2023.

[25]"How Is the Doppler Effect Related to Understanding the Universe?: Socratic." *Socratic.Org*, 26 Aug. 2015, socratic.org/questions/how-is-the-doppler-effect-related-to-understanding-the-universe.

[26]"Obtaining Astronomical Spectra- Spectrographs." *Obtaining Astronomical Spectra- Spectrographs*, 7 June 2023, www.atnf.csiro.au/outreach/education/senior/astrophysics/spectrographs.html.

[27]"The Relativistic Doppler Effect." *Apache2 Ubuntu Default Page: It Works*, spiff.rit.edu/classes/phys314/lectures/doppler/doppler.html. Accessed 3 Aug. 2023.

[28]"Astronomical Redshift." *Imaging the Universe - The University of Iowa*, itu.physics.uiowa.edu/labs/advanced/astronomical-redshift. Accessed 3 Aug. 2023.

[29]Staff, Prisha Singh- CuriouSTEM. "Theories in Physics: Hubble's Law." *CuriouSTEM*, 11 Nov. 2020, www.curioustem.org/stem-articles/theories-in-physics-hubbles-law1.

[30]Warren, Sasha. "The Hubble Constant, Explained." *University of Chicago News*, news.uchicago.edu/explainer/hubble-constant-explained. Accessed 3 Aug. 2023.

[31]"What Is Gravitational Lensing?" *EarthSky*, 8 Sept. 2021, earthsky.org/space/what-is-gravitational-lensing-einstein-ring/.